Detection of bone marrow edema in differential diagnoses of odontogenic cysts using dual-energy computed tomography

Hasegawa, Takumi ; Arimoto, Satomi ; Saito, Izumi ; Yatagai, Nanae ; Murakami, Aki ; Sasaki, Aki ; Tadokoro, Yoshiaki ; Tani, Wakiko ;…

(Citation)
Oral and Maxillofacial Surgery,27(4):675-684

(Issue Date)
2023-12

(Resource Type)
journal article

(Version)
Accepted Manuscript

Detection of bone marrow edema in differential diagnosis of odontogenic cysts using dual-energy computed tomography

Takumi Hasegawa, DDS, PhD [1]*, Satomi Arimoto, DDS, PhD[1]†, Izumi Saito, DDS, PhD[1]†, Nanae Yatagai, DDS [1]§, Aki Murakami, DDS [1]§, Aki Sasaki, DDS [1]§, Yoshiaki Tadokoro, DDS [1]§, Wakiko Tani, RT [2]†, Kiyosumi Kagawa, RT [2]†, Masaya Akashi, DDS, PhD[1] ll

* Senior Assistant Professor, §Graduate Fellow, †Clinical Fellow, ll Professor and Chairman

[1] Department of Oral and Maxillofacial Surgery, Kobe University Graduate School of Medicine

[2] Center for Radiology and Radiation Oncology, Kobe University Hospital

*Corresponding author: Takumi Hasegawa, DDS, PhD, Department of Oral and Maxillofacial Surgery, Kobe University Graduate School of Medicine, 7-5-1, Kusunoki-cho, Chuo-ku, Kobe 650-0017, Japan. Tel: +81-78-382-6213 / Fax: +81-78-351-6229

E-mail: hasetaku@med.kobe-u.ac.jp

ABSTRACT

Purpose: In this study, we prospectively investigated the relationship between bone marrow edema (BME) and odontogenic cysts and explored the possibility of using dual-energy computed tomography (DECT) as an auxiliary tool for the diagnosis of odontogenic cysts.

Methods: This cross-sectional study included 73 patients who underwent the DECT scan and surgery for odontogenic cysts or odontogenic tumors. The virtual noncalcium (VNCa) computed tomography (CT) values and CT values were measured at several sites. The predictor variable was diagnosis, and the other variables included age, sex, and sites. The primary outcome was VNCa CT value. Variables were tested using the chi-square test or Kruskal–Wallis test. The VNCa CT and CT values were tested using the Scheffe test for multiple comparisons. All variables were analyzed as independent variables affecting the VNCa CT values around the lesion in the multiple regression analysis.

Result: There were 35 men and 38 women. The mean patient age was 50.0 ± 19.5 years (range: 8–86). The VNCa CT values (-6.2 ± 34.3) around the lesion in patients with RCs were significantly higher than those in patients with dentigerous cysts (-44.4 ± 28.6) and odontogenic keratocysts (-67.3 ± 19.5). In multiple regression analysis, the VNCa CT values around the lesion showed a significant positive correlation with histological results (regression coefficient: -0.605, $P < 0.001$).

Conclusion: The presence of BME is associated with radicular cysts, and DECT can be used as an auxiliary tool for radicular cyst diagnosis.

Key words: prospective, dual-energy computed tomography, odontogenic cysts, bone marrow edema, head and neck

INTRODUCTION

The quality and clinical applications of computed tomography (CT) made remarkable progress by employing computational abilities for iterative reconstructions. Recently, dual-energy CT (DECT) became available in clinical practice. DECT uses two datasets with different energy spectra in contrast to single energy scanning methods that use only one spectrum. Therefore, DECT has several advantages such as visualization and quantification of iodine, automated bone subtraction in CT angiography, detection of perfusion defects caused by pulmonary embolism, and detection of bone marrow edema (BME)[1-5].

BME is not a disease but a general condition arising due to various factors including trauma and hemorrhage in the bone marrow following a bone fracture and inflammation associated with conditions such as osteomyelitis, osteonecrosis, arthritis of the joints, and bone marrow infiltration by tumor cells[6-8]. In the field of orthopedics, BME is a marker for potential disease progression of osteonecrosis of the femoral head and is correlated with worsening pain[9,10]. Hence, early detection of BME is important to predict the deterioration of the patient's condition and worsening of the symptoms. Magnetic resonance imaging (MRI) is the standard diagnostic tool for the detection of BME because the edema cannot be detected using conventional CT[6,11]. However, MRI cannot be routinely used for all patients with cysts because it is expensive, requires long examination time, and has restricted use in patients with claustrophobia and metal implant in the body. Moreover, the complex anatomy and close proximity of various tissues in the head and neck region complicate the diagnosis of BME in this region. However, recently, DECT is being used to visualize subtle bone involvement in osteomyelitis, osteonecrosis, and cancers in the head and neck region[8]. However, further research is needed to investigate whether BME in the head and neck region is reliably detected by DECT. At present, no study has investigated the relationship between BME and odontogenic cysts using DECT.

Odontogenic cysts are categorized into developmental and inflammatory cysts based on their origin. Although odontogenic cysts have various histological types, inflammatory cysts are usually radicular cysts (RCs) and developmental cysts are usually dentigerous cysts (DCs) or odontogenic keratocysts (OKCs)[12-14]. These cysts require different treatment approaches. For example, careful cystectomy is necessary in OKCs because of the high risk of recurrence, and apicoectomy of the teeth involved is necessary in RCs. These cysts sometimes have similar image features on conventional radiographs. Although biopsy is often needed before surgery, repeated invasive procedures impose a burden on the patients and increase the risk of infection. Clinically, there are patients who refuse biopsy for reasons of repeated surgical invasion.

The purpose of this study was to investigate the relationship between BME and odontogenic cysts and explore the possibility of using DECT as an auxiliary tool for diagnosis. We hypothesized that the presence of BME, as detected by DECT, is associated with odontogenic cysts. The specific aims of the study were to compare the virtual noncalcium (VNCa) values among each histopathological diagnosis.

MATERIALS & METHODS

Study design/sample

The investigators designed and conducted a cross-sectional study. This study was approved by the institutional review boards of Kobe University Graduate School of Medicine and the participating hospitals (authorization number: 180191). Each patient was informed about surgery-associated risks and provided consent for using their CT findings. We published information regarding this study, and patients were allowed to opt out of this study anytime. The study population comprised all patients who underwent DECT and surgery for an odontogenic cyst or odontogenic tumor between September 2018 and December 2020 at the Department of Oral and Maxillofacial Surgery of Kobe University Hospital. The inclusion criteria were as follows: cases that were clinically identified as an odontogenic cyst or tumor by orthopantomography, and cases wherein patients underwent DECT and surgery for an odontogenic cyst or odontogenic tumor. The exclusion criteria were as follows: cases wherein DECT or surgery was not performed, cases in which the diameter of the lesion is <5 mm, immeasurable cases involving severe artifacts in BME, cases with little cancellous bone required to measure BME, and cases with recurrent cysts or tumors.

Variables

The predictor variable was histological results. Histological results were classified into four groups (RCs, OCs, OKCs, and others). The primary outcome variable was BME (VNCa CT values). The other variables were sex, age, lesion site (anterior or molar region), and jawbone involved (maxillary or mandible).

Data collection methods

Data assessed for each patient included sex, age, histological results, and lesion site. The investigator obtained the clinical data from electronic medical records. VNCa CT values and CT values were measured. The data obtained for each subject were entered into a data sheet.

The included subjects were examined with a third generation DECT scanner (Somatom Force; Siemens Healthineers, Erlangen, Germany). The scanner was equipped with two X-ray tubes, tube A and tube B. Tube voltages were set at 100 and 150 kVp for the tubes A and B, respectively, and a tin filter was used in the tube B (Sn150 kVp). The predefined tube current–time product ratio was set at 1.6:1 (tube A, 260 quality reference mAs; tube B, 144 quality reference mAs). Three different images were retrieved with each DECT scan: 100 kVp, Sn150 kVp, and weighted average (calculated from the tube A and B data at a ratio of 0.4:0.6) to resemble the contrast properties of a 120-kVp standard CT image. Dual-energy-specific data were obtained by reconstructing the axial sections of the 100 and Sn150 kVp data sets (section thickness 1.0 mm, increment 0.7 mm) with a bone kernel (Br64) and a soft-tissue kernel (Qr40). Postprocessing of the data from the CT images was performed using a software (Syngo, via version VB20A; Siemens Healthineers) with a three-material decomposition algorithm for bone mineral, yellow marrow, and red marrow. The relative contrast ratio was set to a value of 1.53 at 100 and Sn150 kV. The strength of the smoothing filter was set to 2 virtual noncalcium (VNCa) and the reconstructions were created as color-coded images consolidated with weighted average CT images using the BME setting in the Syngo Dual Energy software.

BME on DECT were detected by visual evaluation of the color-coded VNCa reconstruction images. It was represented in purple in the normal and fatty bone marrow with a very low attenuation, and represented in green with increased attenuation in BME (Figure 1). BME was graded from 0–3 (0 = no BME, 1 = mild BME, 2 = moderate BME, and 3 = marked BME) for clinical purposes according to Timmer et al[14]. The quality of the DECT was subjectively classified as 1 = excellent, 2 = good, 3 = moderate, and 4 = poor. The values of VNCa CT and CT (in Hounsfield units [HUs]) were obtained from color-coded VNCa images by using circular region of interests (ROIs) of 5 mm^2 (Figure 2). The values were obtained at horizontal or coronal planes where the lesion had the largest diameter. The VNCa CT values in center of the lesion were defined as “the VNCa CT values in the lesion.” The VNCa CT values measured within 10 mm of the lesion were defined as “the VNCa CT values around the lesion.” When the VNCa CT values could be measured in several point around the lesion, the average values were used as results. The corresponding values from the opposite side of the lesion were defined as “the VNCa CT values in normal bone.” The CT values were measured similar to the VNCa CT values. All the ROIs were placed carefully to avoid strong interference from the root of teeth and the cortical bone.

Statistical analyses

Statistical analyses were performed using SPSS, version 22.0 (IBM Corp., Armonk, NY, USA), and

Ekuseru-Toukei 2012 software (Social Survey Research Information Co., Ltd., Tokyo, Japan). Continuous variables were tested using the Kruskal–Wallis test, and categorical variables were tested using the chi-square test. The VNCa CT values around the lesion among each histological result and the impression of BME were tested using the Scheffe test following the Kruskal–Wallis test for multiple comparisons of ordinal variables. All the variables were analyzed as independent variables affecting the VNCa CT values around the lesion in multiple regression analysis. Variables with a variance inflation factor of greater than 10 were excluded. The data were entered in a multiple regression analysis in which the patients were divided according to the histological results (RCs, OCs, OKCs, and others), lesion site (anterior vs. molar region), and the jawbone involved (maxillary vs. mandible). Probability values of less than 0.05 were considered as being statistically significant.

RESULTS

The study group included 73 patients (35 men and 38 women). Mean patient age was 50.0 ± 19.5 years (range: 8–86). Data of patient variables and the characteristics and histological results of the lesions are shown in Table 1. The most common histological type of the odontogenic cyst was RC with 36 (49.3%) cases. There were 24 (32.9%) cases of DCs and 6 (8.2%) cases of OKCs (Table 1). The representative images of RC, DC, and OKC are shown in Figure 3. The most common lesion site in patients with DCs was the molar region of the mandible (95.8%). Moderate and marked BME in the visual impression were observed only in patients with RCs (Table 1). According to the subjective quality assessment of DECT images, 28 images (38.4%) were excellent, 22 (30.1%) were good, 18 (24.7%) were moderate, and 5 (6.8%) were poor (Table 1). The reasons for moderate- and poor-quality images included artifacts (2 cases) and too little cancellous bone (21 cases) to measure BME. In visual impression of BME, the VNCa CT values around the lesion were -50.7 ± 29.5 HUs, -19.0 ± 35.1 HUs, 5.8 ± 35.0 HUs, and 11.1 ± 20.3 HUs in no, mild, moderate, and marked BME, respectively. The VNCa CT values of mild and marked BME were significantly higher than those of no BME ($P < 0.05$) (Figure 4a). The VNCa CT values of marked BME were significantly higher than those of moderate BME ($P < 0.05$) (Figure 4a). Data of patient variables and the VNCa or CT values are shown in Table 2. The VNCa CT values in the normal bone of the mandible were significantly higher than those of the maxilla (Table 2). The CT values around the legion of the maxilla were significantly higher than those of the mandible (Table 2). Data of histological results and the VNCa or CT values are shown in Table 3. The VNCa CT values and CT values in each histological result are shown in Figures 4b, 4c, 5a, 5b, 5c, and 5d. The VNCa CT values in the lesion and normal bone and the CT values in all measurement sites were not significantly associated with histological results (Figures 4b, 4c, 5a, 5b, 5d). However, the VNCa CT values around the lesion were significantly more in patients with RCs than in patients with DCs and OKCs ($P < 0.05$) (Table 3, Figure 5c).

Table 4 presents the standardized regression coefficients and adjusted R-square for factors affecting the VNCa CT values around the lesion in the multiple regression analysis. The VNCa CT values around the lesion positively correlated with the histological results. The combination of these variables explained 33.3% (low) of the variance in the regression analysis of the VNCa CT values around the lesion.

DISCUSSION

The purpose of this study was to investigate relationship between BME and odontogenic cysts and explore the possibility of using DECT as an auxiliary tool for diagnosis. We hypothesized that the presence of BME, as detected on DECT, is associated with odontogenic cysts. The specific aims of the study were to compare the VNCa values among each histopathological diagnosis. In this study, the VNCa CT values around the lesion in patients with RCs were significantly higher than those in patients with DCs and OKCs. Moreover, moderate and marked BME in the visual impression were observed only in patients with RCs.

The jaw bones have a thick cortical bone and little bone marrow and cancellous bone unlike the spine and the long bones. Additionally, the mandible has a mandibular canal with abundant blood flow. The thick cortical bone (Figure 6) and the mandibular canal (Figure 7) increase the difficulty in obtaining the VNCa CT values and CT values. In this study, the diagnosis of BME in most cases was comparatively easy, although 5 (6.8%) cases were difficult to diagnose. Therefore, it is possible to detect BME in the head and neck despite the unfavorable anatomy of the region. Existence of metal artifacts makes the diagnosis of BME difficult on both DECT and MRI. In particularly, metal artifacts often appear in the head and neck region because of dental restorations, prosthesis, and implants. Virtual monoenergetic imaging reconstructions can be used to reduce metal artifacts, although only 2 cases had severe artifacts in this study[15-17].

Since ancient times, the discrimination diagnosis of an odontogenic cyst or odontogenic tumor was well known using radiographic features. RCs have radiolucent circular areas and continuity with the apex of teeth along with infected or necrotic pulp. DCs have radiolucent circular areas with sclerotic margins around tooth crowns[18]. OKCs have aggressive and infiltrative features with frequent recurrence[19]. OKCs have unicystic or multicystic radiolucent circular areas similar to RCs or DCs[19]. These cysts cannot be well distinguished radiologically; however, a probable diagnosis can be made. For example, if RCs has a large diameter involving multiple teeth, then the diagnosis may be difficult. Therefore, several studies tried to distinguish odontogenic cysts and tumors using CT values (HUs)[20, 21]. HU assessment of CT is widely applied as an easy diagnostic tool for various diseases[22]. Uehara et al. reported the mean HU values of 51.1 ± 11.8 for RCs, 52.8 ± 12.2 for DCs, and 37.9 ± 12.8 for OKCs[20]. Crusoé-Rebello et al reported that the average HU was 28.4 ± 10.5 (-22.9–97.9) for OKCs[21]. Other reports demonstrated 3.9–22.9 HUs for DCs[23, 24]. In this study, the CT values (HUs) in the lesion were 60.2 ± 42.4 for RCs, 44.8 ± 20.8 for DCs, and 57.3 ± 63.3 for OKCs. The CT values of OKCs were higher than those reported in other studies[20, 21]. OKCs have highly viscous content that includes keratin[25]. RCs also have a highly viscous content similar to that of OKCs including cell debris containing proteins and intracellular particles[25]. On the contrary, DCs contain fluid accumulation between reduced enamel epithelium and the tooth crown[25]. The results may be related to the content and viscosity of cystic fluid because protein concentration and viscosity highly affect the CT values[26, 27]. However, careful consideration is needed before generalizing this result because of the small population size and large dispersion of cases.

BME is a prodrome of bone destruction and a prediction marker for worsening of symptoms[9, 10]. It is also one of the first signs of inexplicable pain or teeth mobility[28]. Recently, DECT has not become available in clinical practice to detect BME caused by various diseases[1-5]. It is being used to visualize subtle bone involvement in oncology, osteomyelitis, and osteonecrosis of the head and neck region[8]. The sensitivity and specificity of DECT for the detection of BME with VNCa DECT reconstructions were investigated in numerous studies and were found to be relatively high at 82–96% and 83–98%, respectively[28-30]. Therefore, DECT is a reliable diagnostic tool for the detection of BME. Theoretically, inflammatory cysts such as RCs cause inflammation and BME around the lesion. Developmental cysts such as DCs and OKCs are not expected to cause BME unless infected. However, there has been no study that investigated the relationship between BME and odontogenic cysts. Therefore, the strength of this study was to demonstrate the relationship between BME and odontogenic cysts. In the future, we may be able to distinguish odontogenic cysts with similar image features without needing biopsy. On the contrary, this study had several limitations. First, the present prospective study was an explorative study with a relatively small heterogeneous population. In particular, there were only 6 patients with OKCs. Second, BME may be associated with periapical, periodontal, and preoperative infections. In this study, these causative factors of inflammation were not investigated. Therefore, although the demographic factors did not affect BME in multiple regression analysis, bias could not be completely excluded.

In conclusion, the presence of BME is associated with RCs, and DECT can be used as an auxiliary tool for RC diagnosis. The VNCa CT values around the lesion in patients with RCs were significantly higher than those in patients with DCs and OKCs. Moreover, moderate and marked BME in the visual impression were observed only in patients with RCs. The VNCa CT values and detection of BME may provide additional information to aid the diagnosis in ambiguous cases of odontogenic cysts. Future research using a large-scale cohort and investigating predictors of BME including inflammation should be conducted.

Declarations

Competing interests: Takumi Hasegawa, Satomi Arimoto, Izumi Saito, Nanae Yatagai, Aki Murakami, Aki Sasaki, Yoshiaki Tadokoro, Wakiko Tani, Kiyosumi Kagawa, and Masaya Akashi have no relevant financial or non-financial interests to disclose.

Funding: The authors declare that no funds, grants, or other support were received during the preparation of this manuscript.

Author contribution:

Study design: T Hasegawa, S Arimoto, W Tani, M Akashi

Acquisition of data: T Hasegawa, S Arimoto, I Saito, N Yatagai, A Murakami, A Sasaki, Y Tadokoro

Analysis and interpretation of data: T Hasegawa, S Arimoto, W Tani, K Kagawa

Writing original draft: T Hasegawa

Writing - review & editing: S Arimoto, I Saito, N Yatagai, W Tani, K Kagawa, M Akashi

Statistical analysis: T Hasegawa

Supervision: M Akashi

Project administration: T Hasegawa, M Akashi

Funding acquisition: M Akashi

Ethical Approval:

All procedures performed in studies involving human participants were in accordance with the ethical standards of the institutional committee and with the 1964 Helsinki declaration and its later amendments or comparable ethical standards. Approval was granted by the Ethics Committee of University Kobe University Graduate School of Medicine (Date. 2018/9/18 / No. 180191).

Consent to Participate:

Each patient was informed about surgery-associated risks, and gave their consent for computed tomography.

Instead, the information regarding this study and granted occasions of refusing to participate in this study were published.

Consent to Publish:

All human research participants agreed that the images and information of this study were used as non-personally identifiable information in this study.

Acknowledgements

We thank Editage (https://www.editage.jp/) for editing a draft of this manuscript.

REFERENCES

[1] Pache G, Krauss B, Strohm P, Saueressig U, Blanke P, Bulla S, Schäfer O, Helwig P, Kotter E, Langer M, Baumann T. Dual-energy CT virtual noncalcium technique: detecting posttraumatic bone marrow lesions--feasibility study. Radiology. 2010 Aug;256(2):617-24.

[2] Reagan AC, Mallinson PI, O'Connell T, McLaughlin PD, Krauss B, Munk PL, Nicolaou S, Ouellette HA. Dual-energy computed tomographic virtual noncalcium algorithm for detection of bone marrow edema in acute fractures: early experiences. J Comput Assist Tomogr. 2014 Sep-Oct;38(5):802-5.

[3] Schulz B, Kuehling K, Kromen W, Siebenhandl P, Kerl MJ, Vogl TJ, Bauer R. Automatic bone removal technique in whole-body dual-energy CT angiography: performance and image quality. AJR Am J Roentgenol. 2012 Nov;199(5):W646-50.

[4] Watanabe Y, Uotani K, Nakazawa T, Higashi M, Yamada N, Hori Y, Kanzaki S, Fukuda T, Itoh T, Naito H. Dual-energy direct bone removal CT angiography for evaluation of intracranial aneurysm or stenosis: comparison with conventional digital subtraction angiography. Eur Radiol. 2009 Apr;19(4):1019-24.

[5] Bauer RW, Kerl JM, Weber E, Weisser P, Korkusuz H, Lehnert T, Jacobi V, Vogl TJ. Lung perfusion analysis with dual energy CT in patients with suspected pulmonary embolism--influence of window settings on the diagnosis of underlying pathologies of perfusion defects. Eur J Radiol. 2011 Dec;80(3):e476-82.

[6] Vogler JB 3rd, Murphy WA. Bone marrow imaging. Radiology. 1988 Sep;168(3):679-93.

[7] Hayes CW, Conway WF, Daniel WW. MR imaging of bone marrow edema pattern: transient osteoporosis, transient bone marrow edema syndrome, or osteonecrosis. Radiographics. 1993 Sep;13(5):1001-11; discussion 1012.

[8] Roele ED, Timmer VCML, Vaassen LAA, van Kroonenburgh AMJL, Postma AA. Dual-Energy CT in Head and Neck Imaging. Curr Radiol Rep. 2017;5(5):19.

[9] Iida S, Harada Y, Shimizu K, Sakamoto M, Ikenoue S, Akita T, Kitahara H, Moriya H. Correlation between bone marrow edema and collapse of the femoral head in steroid-induced osteonecrosis. AJR Am J Roentgenol. 2000 Mar;174(3):735-43.

[10] Ito H, Matsuno T, Minami A. Relationship between bone marrow edema and development of symptoms

in patients with osteonecrosis of the femoral head. AJR Am J Roentgenol. 2006 Jun;186(6):1761-70.

[11] Ragab Y, Emad Y, Abou-Zeid A. Bone marrow edema syndromes of the hip: MRI features in different hip disorders. Clin Rheumatol. 2008 Apr;27(4):475-82.

[12] Soluk-Tekkeşin M, Wright JM. The World Health Organization Classification of Odontogenic Lesions: A Summary of the Changes of the 2017 (4th) Edition. Turk Patoloji Derg. 2018;34(1).

[13] Prockt AP, Schebela CR, Maito FD, Sant'Ana-Filho M, Rados PV. Odontogenic cysts: analysis of 680 cases in Brazil. Head Neck Pathol. 2008 Sep;2(3):150-6.

[14] Shear M. Developmental odontogenic cysts. An update. J Oral Pathol Med. 1994 Jan;23(1):1-11.

[15] Guggenberger R, Winklhofer S, Osterhoff G, Wanner GA, Fortunati M, Andreisek G, Alkadhi H, Stolzmann P. Metallic artefact reduction with monoenergetic dual-energy CT: systematic ex vivo evaluation of posterior spinal fusion implants from various vendors and different spine levels. Eur Radiol. 2012 Nov;22(11):2357-64.

[16] Bongers MN, Schabel C, Thomas C, Raupach R, Notohamiprodjo M, Nikolaou K, Bamberg F. Comparison and Combination of Dual-Energy- and Iterative-Based Metal Artefact Reduction on Hip Prosthesis and Dental Implants. PLoS One. 2015 Nov 24;10(11):e0143584.

[17] Bamberg F, Dierks A, Nikolaou K, Reiser MF, Becker CR, Johnson TR. Metal artifact reduction by dual energy computed tomography using monoenergetic extrapolation. Eur Radiol. 2011 Jul;21(7):1424-9.

[18] Tsukamoto G, Sasaki A, Akiyama T, Ishikawa T, Kishimoto K, Nishiyama A, Matsumura T. A radiologic analysis of dentigerous cysts and odontogenic keratocysts associated with a mandibular third molar. Oral Surg Oral Med Oral Pathol Oral Radiol Endod. 2001 Jun;91(6):743-7.

[19] Chrcanovic BR, Gomez RS. Recurrence probability for keratocystic odontogenic tumors: An analysis of 6427 cases. J Craniomaxillofac Surg. 2017 Feb;45(2):244-251.

[20] Uehara K, Hisatomi M, Munhoz L, Kawazu T, Yanagi Y, Okada S, Takeshita Y, Saito EA, Asaumi J. Assessment of Hounsfield unit in the differential diagnosis of odontogenic cysts. Dentomaxillofac Radiol. 2021 Feb 1;50(2):20200188.

[21] Crusoé-Rebello I, Oliveira C, Campos PS, Azevedo RA, dos Santos JN. Assessment of computerized tomography density patterns of ameloblastomas and keratocystic odontogenic tumors. Oral Surg Oral

Med Oral Pathol Oral Radiol Endod. 2009 Oct;108(4):604-8.
[22] Lamba R, McGahan JP, Corwin MT, Li CS, Tran T, Seibert JA, Boone JM. CT Hounsfield numbers of soft tissues on unenhanced abdominal CT scans: variability between two different manufacturers' MDCT scanners. AJR Am J Roentgenol. 2014 Nov;203(5):1013-20.
[23] Cankurtaran CZ, Branstetter BF 4th, Chiosea SI, Barnes EL Jr. Best cases from the AFIP: ameloblastoma and dentigerous cyst associated with impacted mandibular third molar tooth. Radiographics. 2010 Sep;30(5):1415-20.
[24] Martinelli-Kläy CP, Martinelli CR, Martinelli C, Macedo HR, Lombardi T. Unusual Imaging Features of Dentigerous Cyst: A Case Report. Dent J (Basel). 2019 Aug 1;7(3):76.
[25] Eida S, Hotokezaka Y, Katayama I, Ichikawa Y, Tashiro S, Sumi T, Sumi M, Nakamura T. Apparent diffusion coefficient-based differentiation of cystic lesions of the mandible. Oral Radiol 2012; 28: 109–14.
[26] Yoshiura K, Higuchi Y, Ariji Y, Shinohara M, Yuasa K, Nakayama E, Ban S, Kanda S. Increased attenuation in odontogenic keratocysts with computed tomography: a new finding. Dentomaxillofac Radiol. 1994 Aug;23(3):138-42.
[27] Yonetsu K, Bianchi JG, Troulis MJ, Curtin HD. Unusual CT appearance in an odontogenic keratocyst of the mandible: case report. AJNR Am J Neuroradiol. 2001 Nov-Dec;22(10):1887-9.
[28] Timmer VCML, Kroonenburgh AMJLV, Henneman WJP, Vaassen LAA, Roele ED, Kessler PAWH, Postma AA. Detection of Bone Marrow Edema in the Head and Neck With Dual-Energy CT: Ready for Clinical Use? AJR Am J Roentgenol. 2020 Apr;214(4):893-899.
[29] Yang P, Wu G, Chang X. Diagnostic accuracy of dual-energy computed tomography in bone marrow edema with vertebral compression fractures: A meta-analysis. Eur J Radiol. 2018 Feb;99:124-129.
[30] Suh CH, Yun SJ, Jin W, Park SY, Ryu CW, Lee SH. Diagnostic Performance of In-Phase and Opposed-Phase Chemical-Shift Imaging for Differentiating Benign and Malignant Vertebral Marrow Lesions: A Meta-Analysis. AJR Am J Roentgenol. 2018 Oct;211(4):W188-W197.

TABLE CAPTIONS

Table 1. Characteristics and histological results for patients (n = 73)

Table 2. Characteristics and the VNCa or the CT values for patients (n = 73)

Table 3. Histological results and the VNCa or the CT values for patients (n = 73)

Table 4. Standardized regression coefficients for factors affecting the VNCa CT values around the lesion.

FIGURE CAPTIONS

Fig. 1—The color-coded VNCa reconstruction images and BME.

Fig. 2—The points of measurement of the values of VNCa CT and CT.

Fig. 3—The representative images of RC, DC, and OKC.

RC: A case of radicular cyst in right molar region of mandible

DC: A case of dentigerous cyst in incisal region of maxilla

OKC: A case of odontogenic keratocyst in right molar region of mandible

Fig. 4a—The VNCa CT values around the lesion in each visual impression of BME

0 = no BME, 1 = mild BME, 2 = moderate BME, 3 = marked BME

Fig. 4b—The VNCa CT values in normal bone and histological results.

Fig. 4c—The CT values in normal bone and histological results

Fig. 5a—The VNCa CT values in the lesion and histological results.

Fig. 5b—The CT values in the lesion and histological results.

Fig. 5c—The VNCa CT values around the lesion and histological results.

Fig. 5d—The CT values around the lesion and histological results.

Fig. 6—A case of thick cortical bone which is difficulty to measure.

Fig. 7—Image of mandibular canal on DECT.

FIGURE LEGENDS: None

Table 1. Characteristics and histological results for patients (n = 73)

Variables	RC	DC	OKC	Others	Total	P value
Sample size (n; %)	36 (49.3)	24 (32.9)	6 (8.2)	7 (9.6)	73 (100.0)	
Sex						
Male	17 (47.2)	12 (50.0)	5 (83.3)	1 (14.3)	35 (47.9)	0.101
Female	19 (52.8)	12 (50.0)	1 (16.7)	6 (85.7)	38 (52.1)	
Age						
Range	23–86	19–75	18–77	8–72	8–86	0.040
Mean ± SD	56.4 ± 18.6	46.5 ± 15.7	50.5 ± 22.2	33.7 ± 24.7	50.5 ± 19.5	
Jawbone						
Maxillary	20 (55.6)	1 (4.2)	2 (33.3)	2 (28.6)	25 (34.2)	0.029
Mandible	16 (44.4)	23 (95.8)	4 (66.7)	5 (71.4)	48 (65.8)	
Site						
Anterior region	11 (30.6)	1 (4.2)	3 (50.0)	1 (14.3)	16 (21.9)	< 0.001
Molar region	25 (69.4)	23 (95.8)	3 (50.0)	6 (85.7)	57 (78.1)	
The impression of BME around the lesion						
Indicated no BME	1 (2.8)	19 (79.2)	4 (66.7)	7 (100.0)	31 (42.5)	< 0.001
Mild	22 (61.1)	5 (20.8)	2 (33.3)	0 (0)	29 (39.7)	
Moderate	10 (27.8)	0 (0)	0 (0)	0 (0)	10 (13.7)	
Marked	3 (8.3)	0 (0)	0 (0)	0 (0)	3 (4.1)	
Subjective Quality Assessment in DECT images						

Excellent	13 (36.1)	11 (45.8)	2 (33.3)	2 (28.6)	28 (38.4)	0.888
Good	12 (33.3)	7 (29.2)	2 (33.3)	1 (14.3)	22 (30.1)	
Moderate	9 (25.0)	5 (20.8)	1 (16.7)	3 (42.9)	18 (24.7)	
Poor	2 (5.6)	1 (4.2)	1 (16.7)	1 (14.3)	5 (6.8)	

Continuous variable: Kruskal-Wallis test, Categorical variables: chi-squared test

Table 2. Characteristics and the VNCa or the CT values for patients (n = 73)

Variables	The VNCa values						The CT values					
	in normal bone	P value	in the lesion	P value	around the lesion	P value	in normal bone	P value	in the lesion	P value	around the lesion	P value
Sex (Mean ± SD)												
Male	-51.7 ± 31.1	0.463	36.4 ± 59.5	0.732	-25.4 ± 38.0	0.540	213.9 ± 110.6	0.304	58.2 ± 44.9	0.804	214.6 ± 113.6	0.193
Female	-60.8 ± 16.0		31.2 ± 84.5		-30.0 ± 39.4		191.4 ± 118.3		63.1 ± 63.9		183.7 ± 115.4	
Age (regression coefficients)	-0.08	0.641	0.616	0.164	0.372	0.110	0.03	0.970	-0.05	0.878	- 0.13	0.855
Jawbone (Mean ± SD)												
Maxillary	-66.9 ± 31.2	0.035	15.0 ± 98.3	0.083	-20.0 ± 46.0	0.361	216.4 ± 102.9	0.419	47.5 ± 32.5	0.123	243.8 ± 104.3	0.016
Mandible	-50.8 ± 26.0		43.4 ± 54.6		-31.9 ± 33.8		194.8 ± 120.4		67.7 ± 63.2		175.0 ± 113.9	
Site (Mean ± SD)												
Anterior region	-65.1 ± 36.5	0.298	17.6 ± 123.3	0.862	-15.7 ± 54.3	0.361	226.4 ± 106.4	0.347	32.8 ± 17.1	< 0.001	247.4 ± 102.4	0.063
Molar region	-53.8 ± 26.0		38.2 ± 52.1		-31.2 ± 32.6		195.4 ± 116.6		68.7 ± 59.7		184.8 ± 115.1	

Age: t test, Sex, Jawbone, Site, and Histological results: Kruskal-Wallis test

Table 3. Histological results and the VNCa or the CT values for patients (n = 73)

Variables	The VNCa values						The CT values					
	in normal bone	P value	in the lesion	P value	around the lesion	P value	in normal bone	P value	in the lesion	P value	around the lesion	P value
Histological results (Mean ± SD)												
RC	-62.6 ± 27.7	0.375	30.8 ± 38.6	0.012	-6.2 ± 34.3	< 0.001	240.2 ± 108.0	0.027	60.2 ± 42.4	0.272	230.1 ± 119.3	0.092
DC	-47.6 ± 28.4		62.6 ± 67.7		-44.4 ± 28.6		162.6 ± 115.2		44.8 ± 20.8		163.5 ± 106.2	
OKC	-63.7 ± 19.3		22.3 ± 59.6		-67.3 ± 19.5		146.6 ± 91.6		57.3 ± 63.3		146.7 ± 88.3	
Other	-47.3 ± 36.4		-40.8 ± 158.0		-48.1 ± 39.3		190.3 ± 114.5		121.9 ± 125.6		200.7 ± 108.0	

Kruskal-Wallis test

Table 4. Standardised regression coefficients for factors affecting the VNCa CT values around the lesion.

The variables	Regression coefficients	P value
Age	0.025	0.823
Sex	0.076	0.469
Histological results	-0.605	< 0.001
Site	-0.119	0.291
Jawbone	0.179	0.151
Adjusted R^2	0.333	

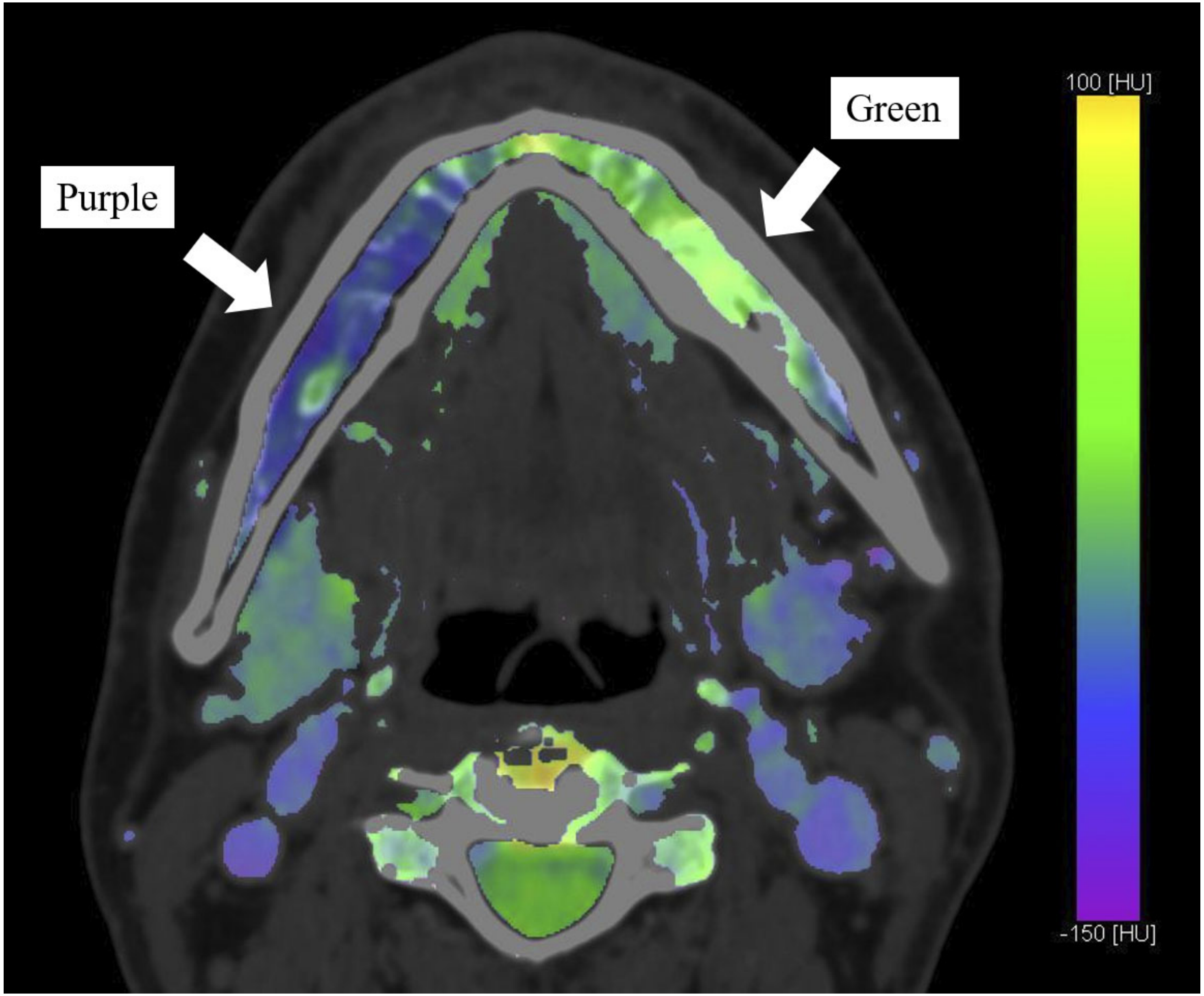
Purple
Green
100 [HU]
-150 [HU]

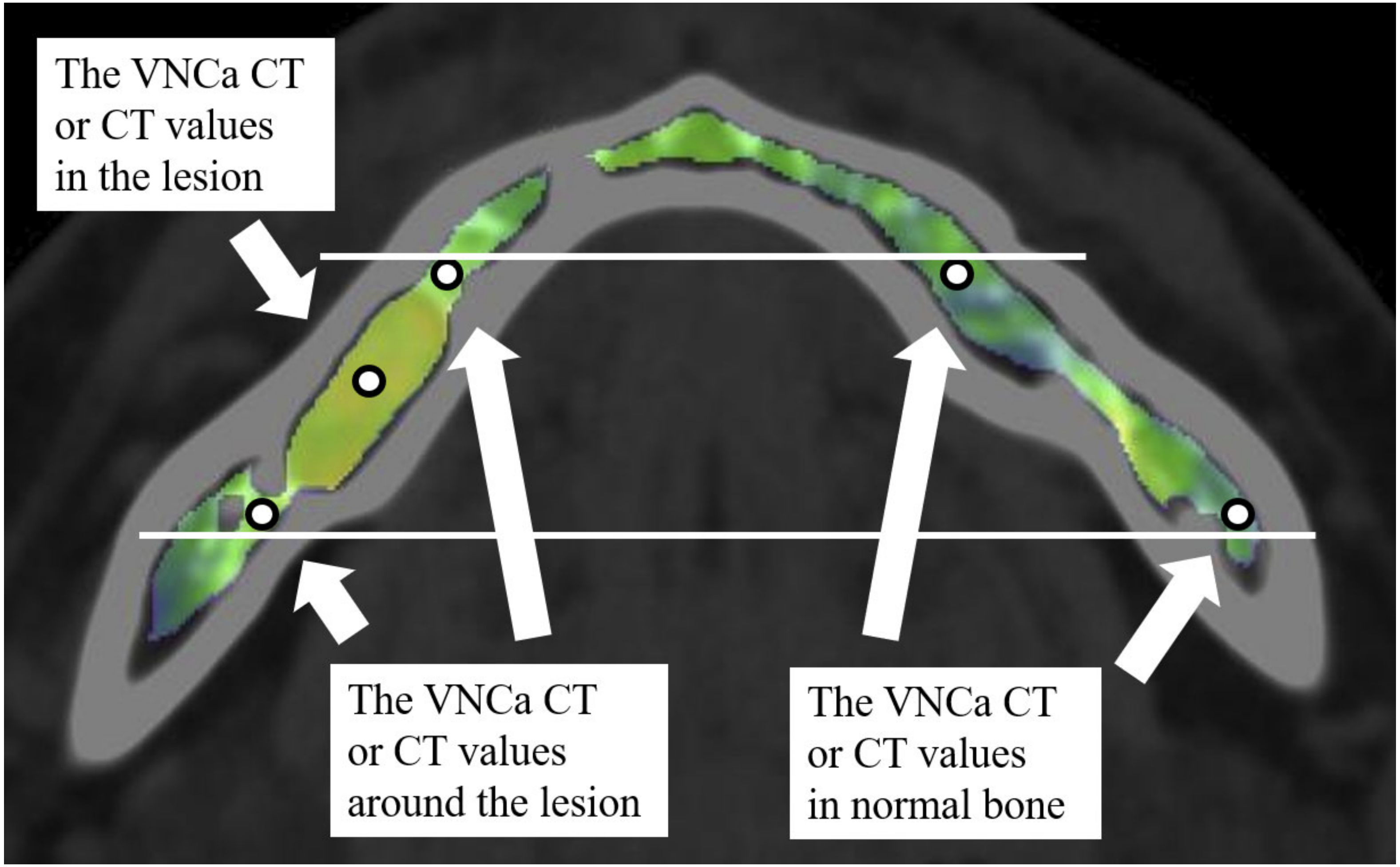
The VNCa CT or CT values in the lesion
The VNCa CT or CT values around the lesion
The VNCa CT or CT values in normal bone

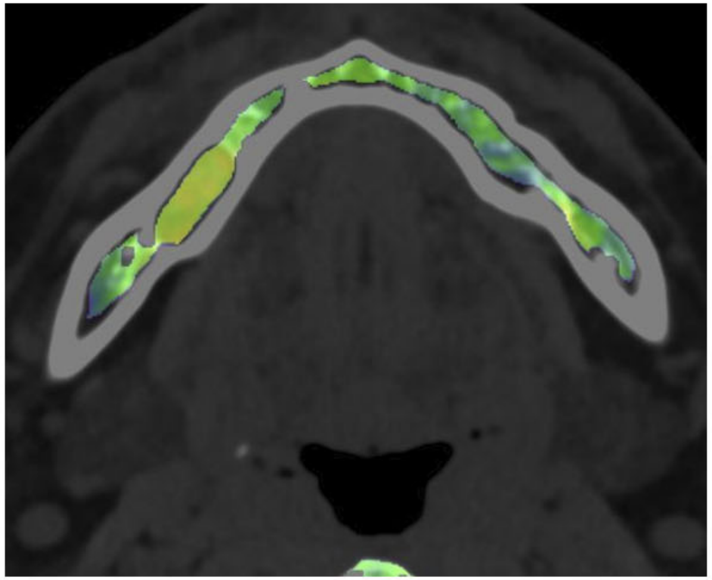

RC

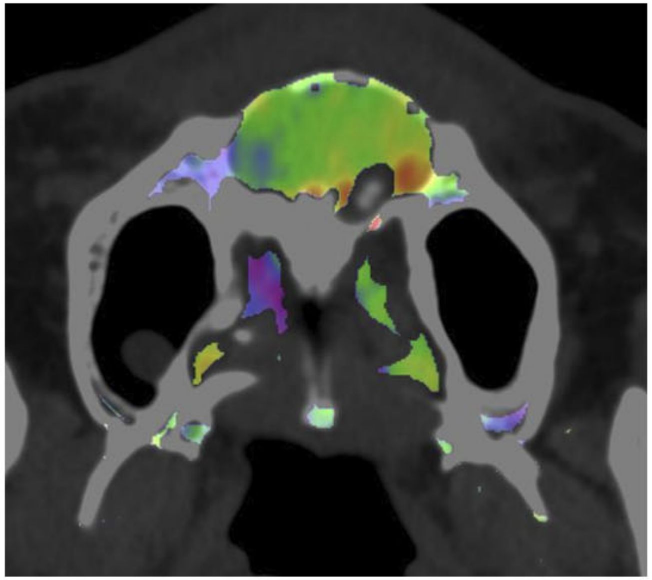

DC

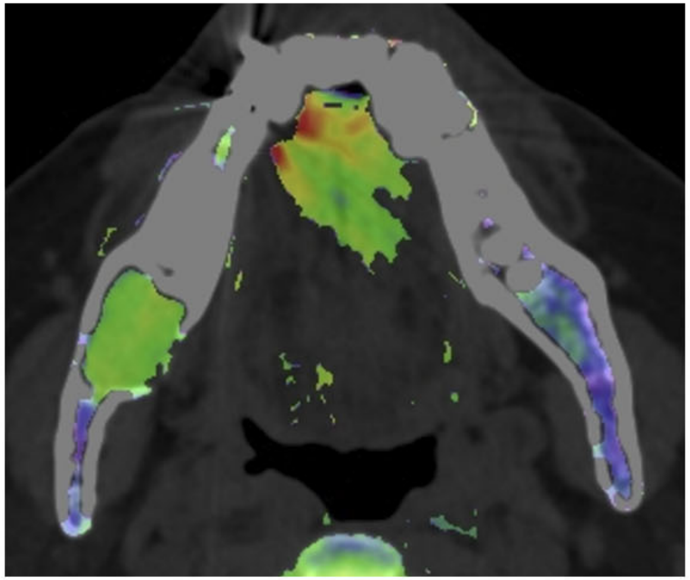

OKC

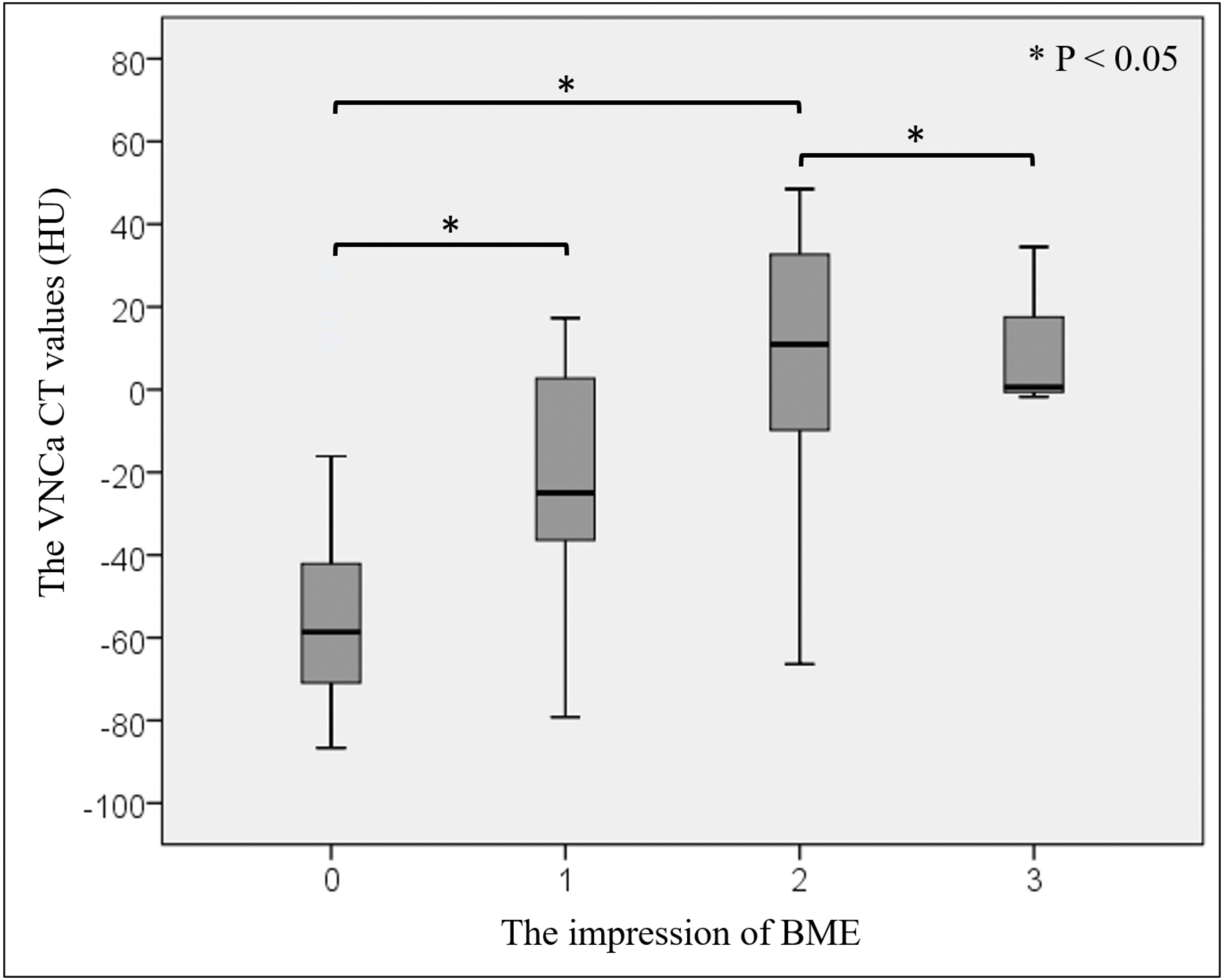

* P < 0.05
*
*
*
80
60
40
20
0
-20
-40
-60
-80
-100
The VNCa CT values (HU)
0
1
2
3
The impression of BME

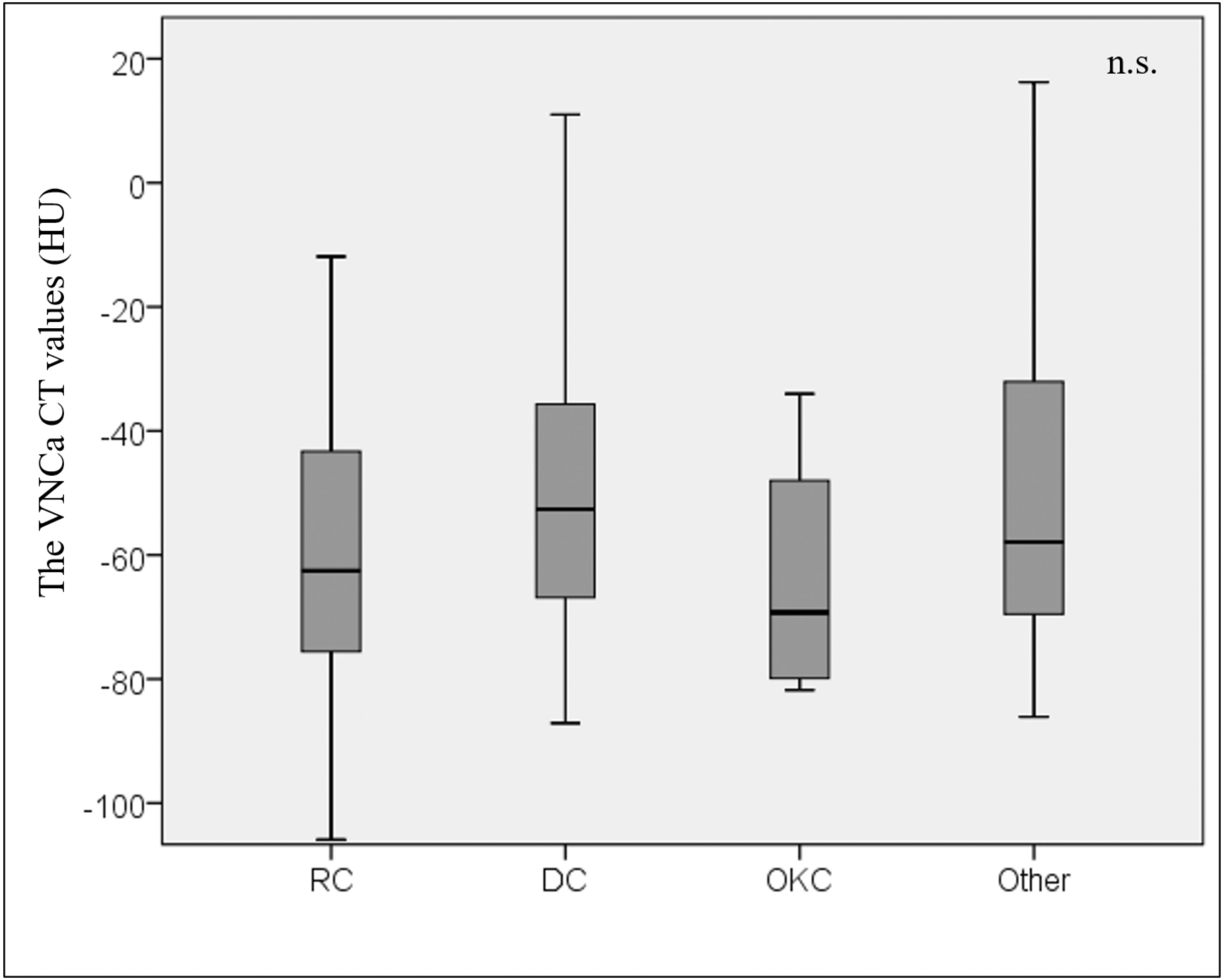

n.s.
20
0
-20
-40
-60
-80
-100
The VNCa CT values (HU)
RC
DC
OKC
Other

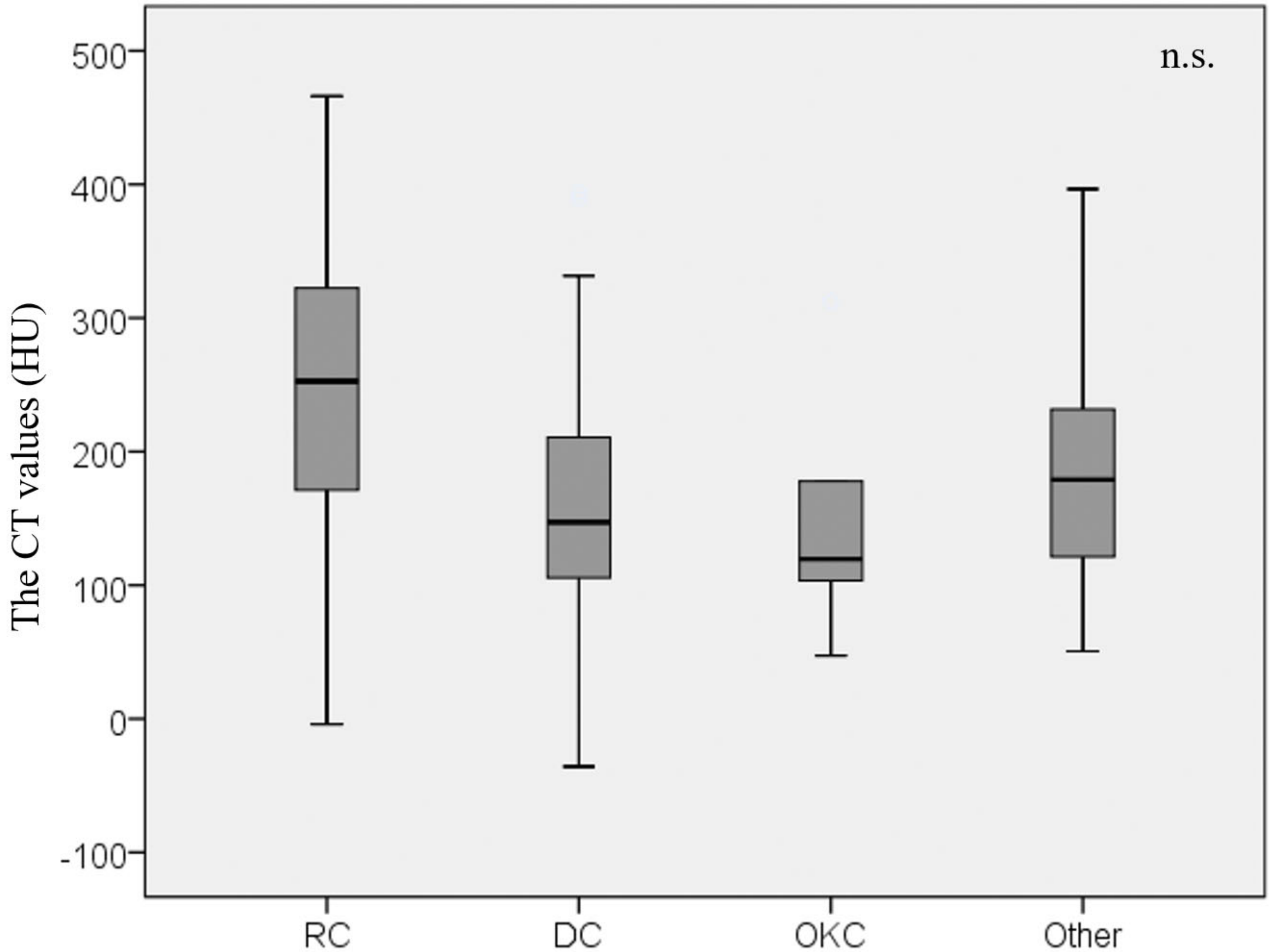

n.s.
The CT values (HU)
500
400
300
200
100
0
-100
RC
DC
OKC
Other

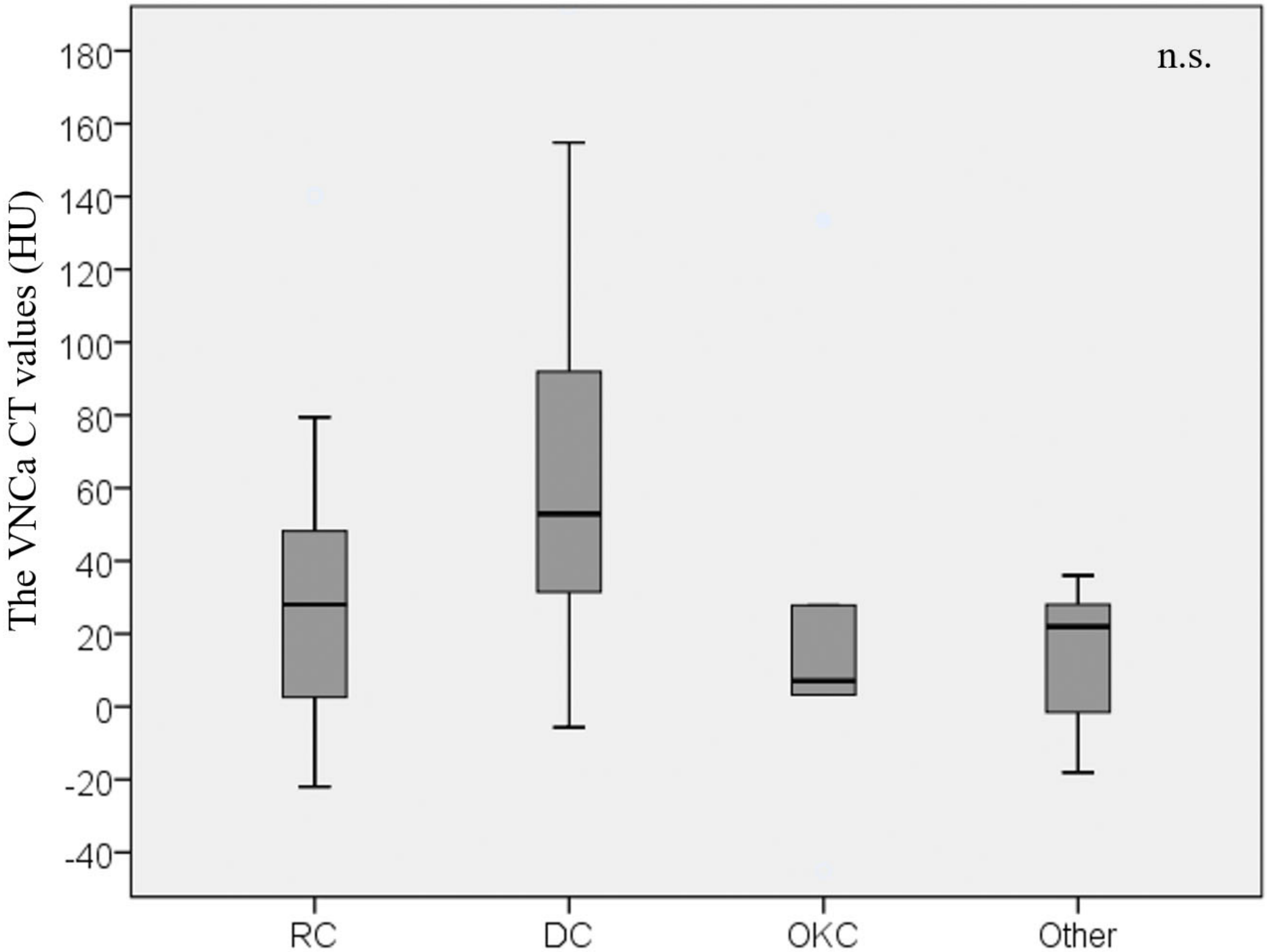

n.s.
The VNCa CT values (HU)
180
160
140
120
100
80
60
40
20
0
-20
-40
RC
DC
OKC
Other

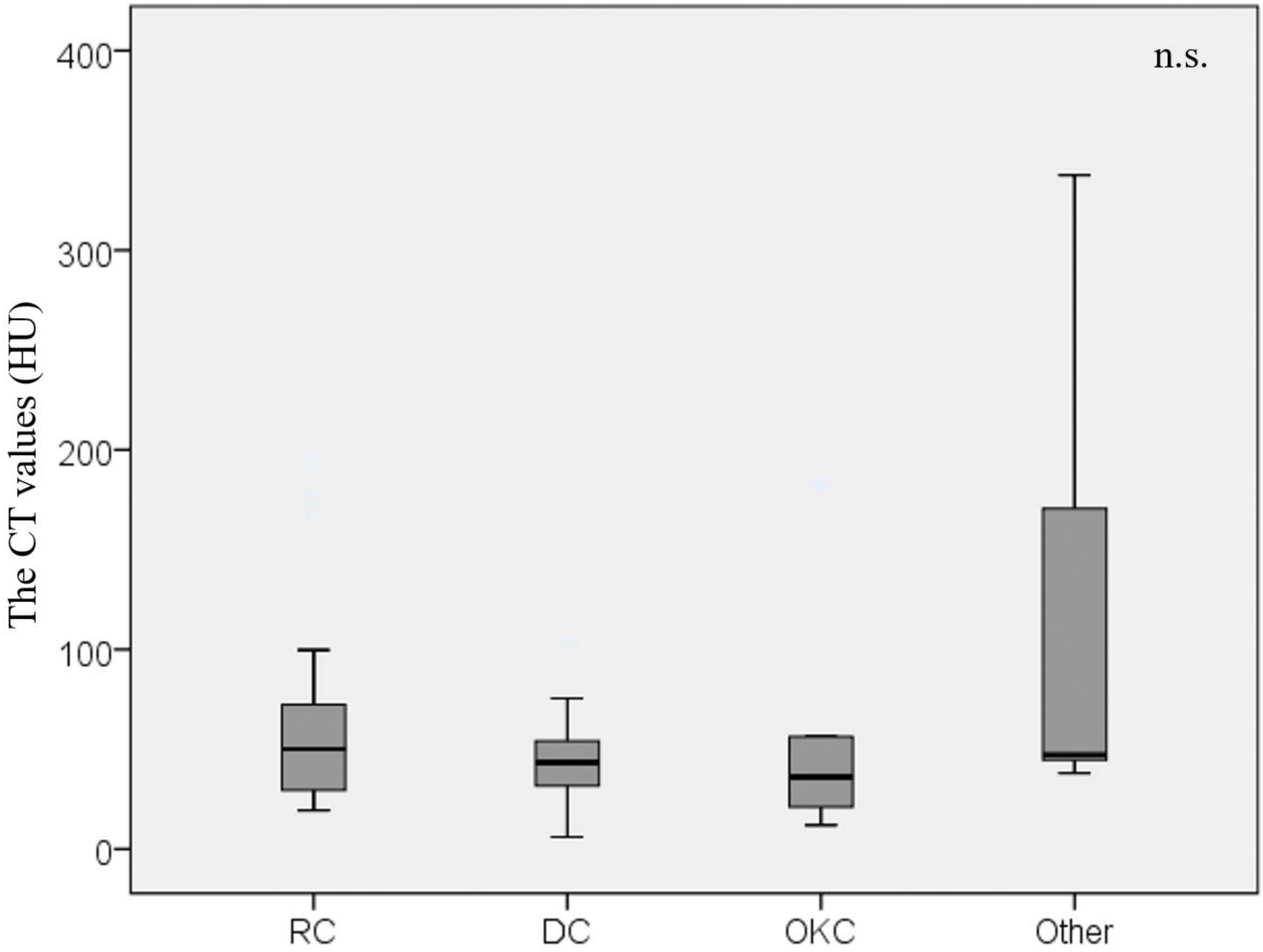

n.s.
The CT values (HU)
400
300
200
100
0
RC
DC
OKC
Other

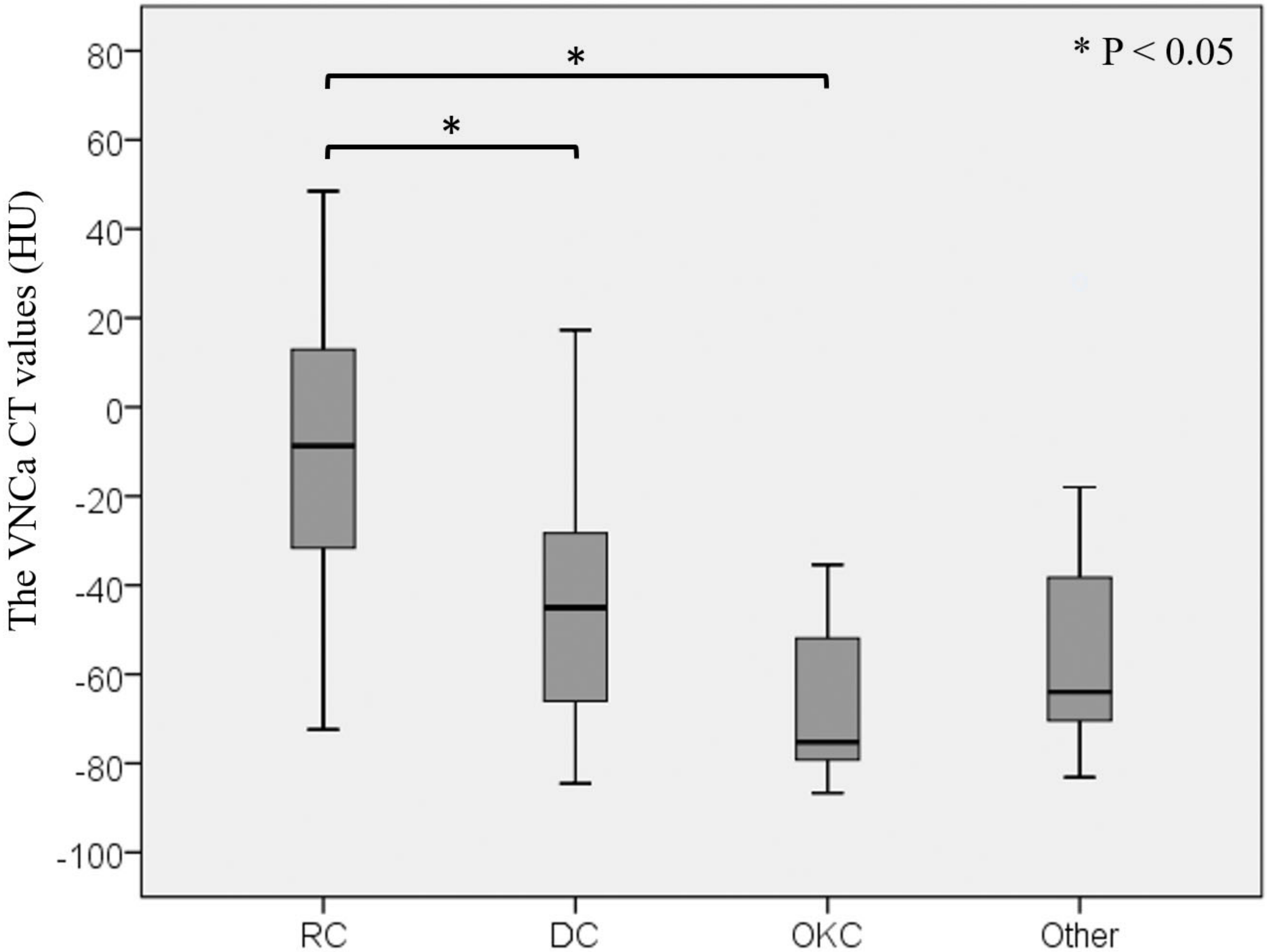

* P < 0.05
*
*
80
60
40
20
0
-20
-40
-60
-80
-100
The VNCa CT values (HU)
RC
DC
OKC
Other

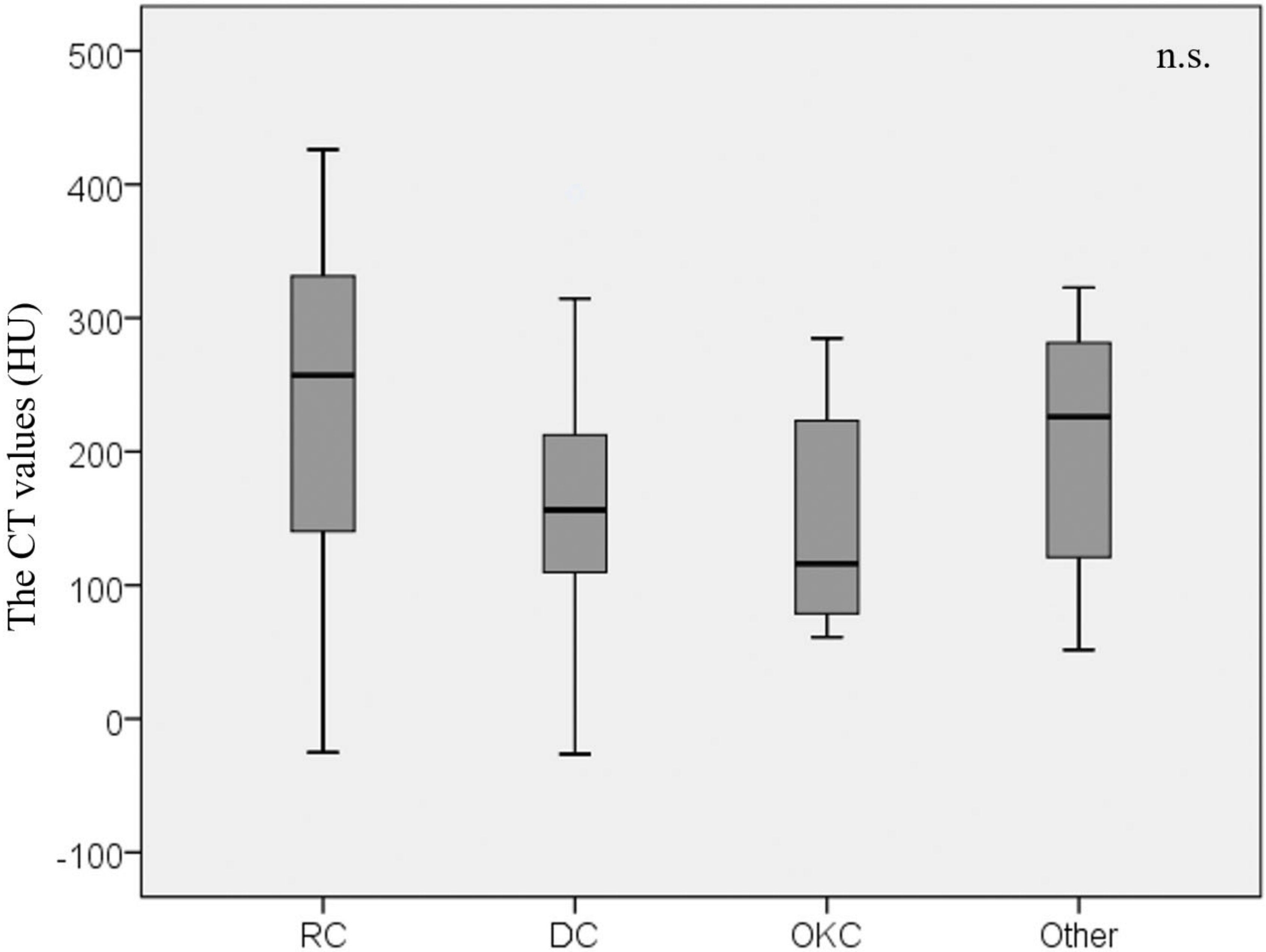
n.s.
The CT values (HU)
500
400
300
200
100
0
-100
RC
DC
OKC
Other